Structuring Cu/ZnO/Al₂O₃ catalyst for methanol synthesis: Slurry additive effect in the washcoating method

Iñigo Pérez-Miqueo, Oihane Sanz [*], Mario Montes

Department Applied Chemistry, Faculty of Chemistry, University of the Basque Country (UPV/EHU), Donostia-San Sebastián 20018, Spain

ARTICLE INFO

ABSTRACT

The best slurry formulation to prepare a structured catalyst for methanol synthesis reaction by washcoating method was investigated. The effect of different inorganic oxide colloids in the slurry preparation of Cu/ZnO/Al₂O₃ catalyst was studied: colloidal ZnO, SiO₂, and Al₂O₃. The addition of all these colloids showed an improvement in adherence obtained on Fecralloy® monoliths, but Al₂O₃ exhibited the best performance. Adherence >80% was obtained with a lower amount of Al₂O₃ than with the other colloids. Nevertheless, the addition of these additives changes the catalytic properties of the parent catalyst. Adding a high amount of colloids decreases the copper metallic surface area which is the active phase of the methanol synthesis reaction. Moreover, the addition of Al₂O₃ gave rise to the dehydration of methanol to dimethyl ether (DME) due to the high acidity that Al₂O₃ presents. Something similar happens but to a less extent with SiO₂, which present weak acidity. In contrast, the basic character of ZnO neutralizes the parent catalyst's low acidity reducing the selectivity to DME. Finally, the slurry formulation containing 10% Al₂O₃ exhibited the best methanol yield. Hence, a methanol synthesis structured catalyst was successfully prepared with similar activity to the powder catalyst.

1. Introduction

Methanol is one of the most demanded products worldwide, of which 30-40 million tons per year are produced by syngas [1,2]. Methanol is widely used in the chemical industry as an intermediate or raw material for many oxygenated compounds (such as formaldehyde, dimethyl ether, formic acid, methyl tert-butyl ether, and acetic acid) and several solvents. It is also employed to synthesise hydrocarbons (especially olefins in a so-called Methanol-to-Olefins (MTO) process). In addition, it can be used for *in situ* easy production of H₂ and itself, as a clean fuel [3, 4].

Copper is the main active metal employed for methanol synthesis. Especially, Cu/ZnO-based catalysts are used [5,6], but since ICI patented a novel catalyst containing Cu/ZnO/Al₂O₃ in 1965 [7], it has been the most common catalyst selected for methanol synthesis reaction due its welcome combination of low prize and high activity [8,9]. Cu is commonly regarded as the active phase, but ZnO and Al₂O₃ have a role that surpasses those of just an inert support [6]. Prašnikar et al. [6] observed that an increased methanol synthesis activity with the uncovering of Al₂O₃ from Cu, indicating a steric hindrance of Cu-Zn active sites. Therefore, the catalytic site Zn sites need to be surrounded by Cu atoms, which are necessary for H₂ activation.

This reaction is traditionally carried out in fixed bed reactors [10]. However, this technology produces high-pressure drops and offers poor heat transfer. Due to the high sensitivity of Cu to temperature, which could deactivate the catalyst by sintering, a considerable effort has been made to control the temperature of this exothermic reaction: the reaction is quenched by adding cold gas at several points or using multi-tubular cooling systems [7,11]. Metallic structured substrates offer interesting possibilities for these tasks. They present a high void fraction and surface/volume ratio, allowing high feed flows with lower pressure drop in the system as well as favouring a better temperature control due to the high conductivity provided by the metallic substrate employed [12]. In particular, the highly conductive substrate offers high radial and axial effective thermal conductivities [13]. Therefore, technologies based on metallic monoliths, foams and microchannel reactors are becoming a promising way of process intensification for exothermic/endothermic reactions [13–15].

Washcoating is one of the most employed coating methods for different substrates due to its simplicity and versatility [16]. One of the main steps in this method is the slurry preparation of the catalyst. Generally, the solid to be deposited is dispersed in an aqueous or

---

alcoholic medium [17]. Factors such as solid content, particle size, viscosity, or additives are vital for obtaining stable slurries to produce homogeneous coatings [17]. However, it is widely accepted that the difficulty of coating catalysts on a metallic substrate is more considerable than on ceramic ones due to the difference in porosity, surface roughness, and thermal stress [18].

Consequently, some additives are required in the slurry formulation to performance the structured catalyst's preparation well. Among the most used additives are inorganic colloids. These colloidal nanoparticles are employed to stabilize the slurry and as a binder, improving the cohesion and adhesion of the catalyst layer. Furthermore, due to the small size of the colloidal particles, during the coating drying process, these small particles are drawn by capillary forces to the intraparticular points of the parent catalyst particles [19]. Hence, they can create anchoring points between particles and between the particles and the substrate. Therefore, many researchers propose using these inorganic oxide colloids in the slurry formulation.

Zamaro et al. [20] showed an improvement in adherence of zeolites on cordierite honeycomb substrates using colloidal SiO_2. With an addition of 3% wt. ratio with respect to the zeolite, the adherence increased 10–20%. The selected colloid nature depends on its compatibility with the catalyst and the scale of the substrate alloy employed. Echave et al. [17] used colloidal ZnO to deposit PdZnO catalyst on Fecralloy, and Pérez et al. [21] used colloidal SiO_2 to deposit SBA-15 on Fecralloy monoliths, while Peela et al. [22] coated alumina on AISI304 employing colloidal alumina. Milt et al. [23] coated Au/TiO_2 catalyst aided with colloidal alumina on Aluchrom YHf monoliths. This alloy presented whiskers of α-alumina on its surface after the proper pre-treatment. Nevertheless, using these additives improves the coating process, but they could also modify the main properties of the parent catalyst, such as activity, selectivity, or stability [17].

To our knowledge, there is little bibliography about $Cu/ZnO/Al_2O_3$ catalyst structuration for the methanol synthesis reaction. Phan et al. [4] studied different methods to deposit Cu-based catalyst on Fecralloy® monoliths and concluded that the use of a slurry for washcoating is the method that produces the best performances for methanol synthesis. Montebelli et al. [3] also carried out the structuration of $Cu/ZnO/Al_2O_3$ catalyst on metallic open-cell foams. They observed that the activity with respect to the parent catalyst decreased due to the slurry preparation steps, the calcination procedure, or both.

In this work, we studied the effect of different inorganic colloidal oxides (ZnO, SiO_2, and Al_2O_3) in the slurry preparation for the structuration of methanol synthesis catalyst ($Cu/ZnO/Al_2O_3$). Although the washcoating process for the preparation of structured catalysts is well known, the additives have a constant amount in slurry formulations, and the role of these additives has not been studied in detail. Therefore, in this work, we have studied in a more in-depth way the influence of the inorganic colloids used, not only in the structuring process but also its influence on the activity and selectivity of the catalyst. In this way, we tested the adherence of the catalyst layer on Fecralloy® monoliths (coated with different slurry formulations) and the catalytic properties of the samples in the methanol synthesis reaction.

2. Experimental

2.1. Parent catalyst preparation

The standard co-precipitation method was used to synthesize the Cu/ZnO/Al_2O_3 catalyst [24]. A solution of the different metal precursors [$Cu(NO_3)_2 \cdot 3H_2O$ (0.6 M), $Zn(NO_3)_2 \cdot 6H_2O$ (0.3M), and $Al(NO_3)_3 \cdot 9H_2O$ (0.1M); salts provided by Sigma-Aldrich], was added dropwise to a vessel containing water at 343 K. The mixture was fixed to pH 7 with a solution 1 M of Na_2CO_3 (Panreac), used as a precipitant agent, and was aged for one hour under the same conditions (343 K and pH 7).

The obtained precipitate was washed with abundant distilled water. Then it was dried at 373 K overnight and calcined at 663 K and 773 K (2

K/min) for 3 h.

2.2. Structured catalyst preparation

The metallic substrates used were Fecralloy® monoliths of 30 mm length and 16 mm diameter (cell density of 289 and 2360 cpsi), prepared by rolling up corrugated and flat metallic sheets. The manufactured monoliths were cleaned with water and soap, and then with acetone before the thermal treatment at 1173 K (10 K/min) for 22 h. This thermal treatment generated alumina whiskers, providing adequate chemical composition and roughness for sticking to the catalyst layer [25].

The washcoating method was selected for structuring $Cu/ZnO/Al_2O_3$ catalyst. The first step to washcoat structured substrates is preparing stable catalyst slurries to be deposited. The slurries were prepared by mixing using a magnetic stirrer the pre-synthesised $Cu/ZnO/Al_2O_3$ catalyst (CZA) in its dried form to avoid double calcination, an inorganic colloid (Al_2O_3 [Nyacol® AL20], ZnO [Nyacol® DP5370] or SiO_2 [Ludox® TMA Sigma-Aldrich]), polyvinyl alcohol (PVA) (Mowiol® 4-88 Sigma-Aldrich) and distilled water. The solids content of the slurries was fixed to 20% wt. The colloid content with respect to the solid fraction (excluding PVA that disappears after calcination) varied from 0 to 33.3%, maintaining the CZA/PVA mass ratio of 21 (Table 1).

Moreover, the neutralization employing boric acid addition to the slurry formulation was studied to avoid the colloidal compound's dehydration capacity. The acid centers from colloidal alumina are able to dehydrate methanol to DME (not desired product) [26]. The boric acid can avoid forming strong Lewis acid sites or reducing the adsorbate molecules' accessibility [27]. The addition of boric acid (5.7–17.1 mmol H_3BO_3/g Al_2O_3, Sigma-Aldrich) was studied to neutralize the acidity of CZA_17.7%Al_2O_3. Finally, the slurries to ensure a good dispersion of the catalyst particles were sonicated for 10 min and stirred overnight.

The washcoating method (or dip coating) consisted of dipping monoliths in the slurry at a constant speed of 3 cm/min, maintaining it dipped for 1 minute, and withdrawing at the same speed. Then, to remove excess suspension from the channels of the monoliths, they are placed in a centrifuge tube that fits the diameter of the monolith over a hollow support that allows to leave a free zone at the bottom of the tube to collect excess suspension without being in contact with the monolith. Monoliths are centrifuged at 400 rpm for 1 min (Eppendorf Centrifuge 5702). Next, the monolith was dried at 393 K for 30 minutes, and the coating procedure was repeated until 1000 mg were coated. Finally, the coated monoliths were calcined at 673, 723, and 773 K.

Additionally, an aliquot of the catalytic slurry was dried and calcined under the same conditions as coated monoliths to obtain the slurried catalyst. The slurried catalyst represents the solid layer coating on a monolith surface, with similar composition and thermal treatments undergone.

Table 1
Formulation of different slurries prepared.

Name	Slurry formulation				Slurried Catalyst composition	
	CZA (wt.%)	Colloid (wt.%)	PVA (wt.%)	H_2O (wt.%)	CZA (wt.%)	Colloid (wt.%)
CZA_0.0%	19.1	0	0.9	80.0	100	-
CZA_10.0% C*	17.3	1.9	0.8	80.0	90.0	10.0
CZA_17.7% C*	15.85	3.4	0.75	80.0	82.3	17.7
CZA_33.3% C*	12.9	6.5	0.6	80.0	66.7	33.3

* C = Employed colloid; namely, Al_2O_3, ZnO and SiO_2.

2.3. Catalytic test

Methanol synthesis reaction was carried out in a Microactivity Reference lab reactor (PID Eng&Tech). A fixed bed reactor (316 Stainless steel Ø 9 mm ID) with 500 mg of catalyst calcined at 673 K (with a particle size of 300-500 μm) was used. The catalyst was diluted with SiC (Carborundum of 500 μm, VWR) to obtain an isothermal bed of 3 cm in length. Before reaction, the catalyst was reduced at 518 K for 4 h (2 K/min) with 5%H_2 in N_2 stream at atmospheric pressure. The reaction was carried out at 533 K and 4 MPa and was fed with a mixture of 90% syngas (H_2/CO = 2) and 10% N_2 with a space velocity (SV) of 2.55 L_{syngas}/g_{CZA}·h. The products were taken out through a thermostatic line and were analysed with a GC (Agilent 7890A) using TCD (HP-PLOT/Q and HP-MOLESIEVE) and FID (HP-PLOT/Q) detectors.

The coated monoliths (1000 mg of catalyst) calcined at 673 K were tested in the same setup as the powder but in a Hastelloy® reactor of Ø16 mm ID. Three thermocouples were used to measure the radial temperature profile of the monolith, and a thermocouple with a double temperature sensor at two different heights was used to measure the axial gradient (Fig. S1).

2.4. Characterisation techniques

The rheological properties of the slurries were measured in a rotational viscometer at 298 K (TA Instruments AR 1500ex). The viscosity value at the 3400 s^{-1} shear rate was taken into account. The Zeta Potential was measured using a MALVERN Zetasizer 2000 instrument. Solids were dispersed in an aqueous solution of 1 mM NaCl. Then, the pH of the solutions was adjusted with HNO_3 or NH_4OH solutions. Finally, the particle size distribution of the catalyst was measured with a Laser Particle Size Analyzer MALVERN Master Sizer 2000.

An ASAP 2020 of Micromeritics was employed to obtain N_2 Adsorption isotherms. Isotherms were measured at 77 K with previous degas at 453 K during 5 hours. The specific surface area (S_{BET}) was calculated with the BET equation, and the specific pore volume (V) was determined at 0.99 P/Po. The equivalent pore diameter was calculated as $4V/S_{BET}$.

Reactive Frontal Chromatography of N_2O (N_2O-RFC) was used for the copper metallic surface area measurement employing Micromeritics AutoChem II 2920. The previously reduced catalyst (with a flow of 10% H_2/Ar) was submitted to pulses of N_2O at 333 K in He flow. At this temperature, the copper surface was oxidized to Cu_2O (Eq. (1)) [28]

$$2 \cdot Cu + N_2O \rightarrow Cu_2O + N_2 \tag{1}$$

The N_2O was trapped with a cold trap of a mixture of liquid N_2 and acetone, and the amount of N_2 produced was quantified with a TCD detector. The copper metallic surface area was determined by Eq. (2), being the atomic cross-sectional area of copper (d_{Cu}) 0.068 nm^2,

$$S_{Cu} \left(m^2/g \right) = n_{N_2}(mol/g) \cdot 2 \cdot N_A \cdot \frac{d_{Cu}(nm^2/atom)}{10^{18}} \tag{2}$$

X-ray diffraction (XRD) patterns were obtained on a Bruker D8 Advanced with CuKα radiation (λ=1,54 Å) from 5 to 85 °. The CuO average size was estimated using the Scherrer equation at 2θ = 38,5°. This angle is the only one of the most intense peaks that have fewer interferences with other compounds. Metal Cu particle size was determined using the Scherrer equation in the reduced samples at 2θ = 43.3° with in-situ XRD measurements.

Temperature programmed reduction (H_2-TPR) was carried out in AutoChem II 2920 (Micromeritics). A mixture of 10% H_2/Ar was flown through the sample at 313 – 1173 K. H_2 consumption was calculated with a TCD.

The sample's acidity was measured by Ammonia Temperature Programmed Desorption (NH_3-TPD) in an AutoChem II 2920 (Micromeritics). The sample was pretreated at 443 K with He flow for 30 min,

cooled down to 373 K with He, and saturated with ammonia using a flow of 10%NH_3 in He for 15 min. Finally, the adsorbed ammonia was desorbed with a flow of He. A temperature program from 373 to 950 K was employed with a 10 K/min ramp. The signal was recorded with a mass spectrometer, and the 15 m/z signal was followed for NH_3 desorption.

The adherence of the catalytic layer deposited in the monolith was calculated by measuring the weight loss produced during sonication of the coated monolith immersed in petroleum ether (OPPAC) for 30 minutes at room temperature [29].

3. Results and discussion

3.1. The preparation of CZA catalyst slurry

The first step to washcoat structured-substrates is to prepare a stable slurry of the catalyst to be deposited. Water was selected as dispersion media for the CZA catalyst slurry preparation because alcohols produced poorly adherent catalytic layers than that obtained with water [17,30]. To develop a homogeneous and strongly adhered catalyst layer by washcoating, the particle size of catalyst, pH, viscosity, solid contents, and additives, must be adequately adjusted [12,18,19].

Three different inorganic colloids were selected to be used as binders, considering the chemical compatibility between the CZA catalyst and the Fecralloy® monolith surface covered with alumina whiskers. The Al_2O_3 colloid would have affinity with CZA and the monolith surface, the ZnO colloid would have an affinity only with the CZA catalyst, and the colloid SiO_2 will not have a particular affinity with either of the two.

An important parameter in preparing a stable slurry in water is the Z potential of the solids used: catalyst and binders. This variable indicates the suitable pH range to maximize the repulsion between particles to improve the slurry stability. The CZA catalyst showed an isoelectric point at pH values around 10 and a high zeta potential value at pH 6 (Fig. 1). However, using Cu-based catalysts, pH changes must be carefully analysed. As is shown in Fig. 1 (top image), acid solution (pH<4) leads to the dissolution of the copper [31], and the suspension become transparent. However, the use of large amount of ammonia (pH > 11) generate a copper coordination complex and the solution becomes dark blue [32,33].
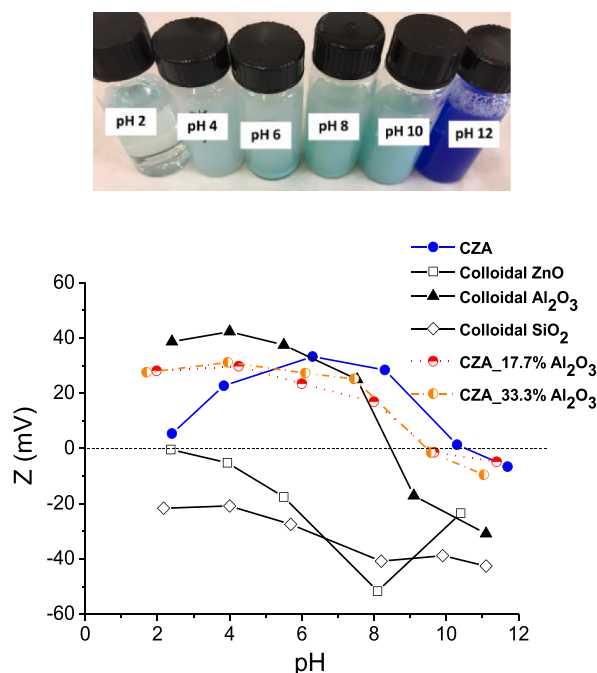

Fig. 1. Zeta potential of different samples at different pH values.

On the other hand, the inorganic oxide colloids presented different zeta potential curves (Fig. 1). The colloidal alumina showed the iso-electric point at pH 8.5 and the colloidal ZnO at pH 2. However, the zeta potential values of colloidal SiO_2 were lower than -20 mV in all the studied pH. Moreover, the colloidal ZnO and SiO_2 exhibited a zeta potential negative in all the studied ranges; and the CZA catalyst and the colloidal Al_2O_3 presented more similar zeta potential with positive values at pH lower than 10 and 8.5 respectively and negatives at higher pH values.

When selecting at what pH the suspensions are prepared, it has been taken into account that mixing two solids with different charges (positive and negative) could generate aggregates when combined due to an attraction of charges. Therefore, the zeta potential of the different slurry formulations was also measured (Table 2, Figs. 1, and S2). It can be seen that the addition of colloidal Al_2O_3 to the slurry generated an intermediate behaviour between the two solids (Fig. 1). On the contrary, the use of the colloidal ZnO and SiO_2, with opposite charges to the CZA catalyst, produced a similar behaviour to that of the colloids (Fig. S2). This suggests that the colloidal particles are surrounding the CZA particles.

During the slurry preparation, the measured pHs of all formulations presented values corresponding to zeta potential (higher than +/- 20 mV, Table 2) high enough to ensure the slurry stability [12]. Therefore, the slurries' pH was not modified.

The particle size measurements are shown in Table 2. The starting catalyst, CZA, has a size of 4.2 microns that increases slightly with the addition of the different colloids studied. However, in all cases, the value does not exceed 10 microns, which is considered the limit value below stable suspensions can be obtained [34].

The viscosity of different slurry formulations was also measured (Table 2). The results showed an increase in the viscosity with the colloid content. Moreover, the nature of the colloid affects this property. The addition of colloidal alumina produced the highest viscosity and the colloidal SiO_2 the lowest value, even lower than the slurry without colloid. However, the adequate viscosity to obtain a homogeneous coating by washcoating on structured substrates usually ranges between 5 and 30 mPa·s (at 3.400 s^{-1}) [18]. Therefore, the viscosity values of slurry formulations were adequate (Table 2).

Therefore, it can be said that the selected formulations and preparation conditions for CZA structuring produced stables slurries adequate, in principle, for washcoat Fecralloy monoliths.

3.2. Effect of the inorganic oxide colloids on monoliths washcoating

Monoliths were coated with different slurries by the washcoating method. The number of catalyst coating required to deposit 1 g of catalyst is presented in Table 2. Results show that the viscosity affects the coating process. More immersions were required to deposit the same amount of catalyst when colloidal SiO_2 was used, presenting the lowest viscosity (Table 2). Low viscosity values produced low loading per immersion.

Moreover, all the studied formulations showed homogeneous coatings without plugged channels (Fig. 2). Fig. 2D appears to indicate a dramatic accumulation of the catalyst in some channels of the monolith. This effect is because, during the suspension excess elimination employing centrifugation, a small accumulation always occurs at the ends of the monolith, which are those observed in this image. However, when monoliths are opened, and the channel is longitudinally analyzed, it can be observed that it is only a punctual effect at the ends of some of the channels in only some monoliths and these accumulations are not quantitatively relevant with respect to the monolith as a whole.

For industrial applications, the mechanical properties of the catalyst are very important. However, at this stage of the research, we believe that the most important point is the stability of the coating. In the preparation of the structured catalysts by the washcoating method, the adherence of the catalyst layer to the monolith is an essential parameter that must be considered to avoid catalyst loss during its handling or use [19]. Adhesion test based on heat shock is sometimes applied as a more extreme manner of adhesion testing of structured catalytic reactors used in automotive applications [35]. Nevertheless, this type of testing is less appropriate for structured reactors to be applied under stationary conditions [19]. Zhao et al. [36] compared the thermal shock test with the ultrasonic test (adhesion calculated as the amount of coating remaining after dipping samples in a bath of a supersonic cleaner). The ultrasonic adhesion test showed, in general, higher weight losses than the thermal shock test, but both methods showed the same trends as a function of the preparation variables.

In this work, the coating adherence obtained by the different slurry formulations (Table 1) was analysed using the ultrasonic test [29]. The catalyst layer adherence on Fecralloy® monoliths as a function of the colloid employed and the calcination temperature is presented in Fig. 3. In the absence of inorganic colloids, the interactions between the CZA particles are insufficient to produce a catalyst layer adequately attached, remaining only around 20% of the catalyst after the test.

A dramatic increase was obtained by adding inorganic colloids as a binder using an adequate amount of colloid but also depending on the calcination temperature (Fig. 3). The adherence improved when increasing the colloid content from 5 to 50 % (Fig. 3). Adherence rises to around 90% with all the colloids used, when the colloid content reaches 33.3%.

The small particle of the colloids (nanoparticles) could fill the interparticle space of the catalyst layer [19]. Thus, the cohesion of the coated layer improves. Moreover, the small size of the colloidal particles (Table 2) allows entering into the substrate roughness, improving the anchorage between the catalyst layer and the monolith. Therefore, adherence is improved by increasing the adhesive and cohesive properties of the catalyst layer and substrate [20].

The alumina was the inorganic oxide that produced the best results in adherence (Fig. 3). It could be due to its compatibility between the CZA

Table 2
Slurries properties.

Sample Name	Solid content (Wt. %)	Slurry pH	Zeta Potential (mV)	Particle size (µm)	Viscosity at 3400 s^{-1} (cP)	Number of coatings to deposit 1 g of catalyst
CZA_0%colloid	20	6.5	+ 32	4.2	7.0	32
CZA_10%Al$_2$O$_3$	20	6.4	+ 22	5.6	8.7	29
CZA_17.7% Al$_2$O$_3$	20	5.7	+ 24	6.6	12	25
CZA_33.3% Al$_2$O$_3$	20	5.5	+ 30	7.3	16	21
CZA_17.7%ZnO	20	8.3	- 23	5.3	8.3	30
CZA_33.3%ZnO	20	8.8	- 30	5.9	10	22
CZA_17.7%SiO$_2$	20	7.5	- 20	7.0	4.8	34
CZA_33.3%SiO$_2$	20	7.7	-28	7.4	5.2	33
Colloidal Al$_2$O$_3$	20*	4.2	+42	0.06-0.09*	14	-
Colloidal ZnO	30*	9.9	-40	0.05*	20	-
Colloidal SiO$_2$	34*	8.0	-32	0.01-0.02*	4.8	-

* Manufacturer information
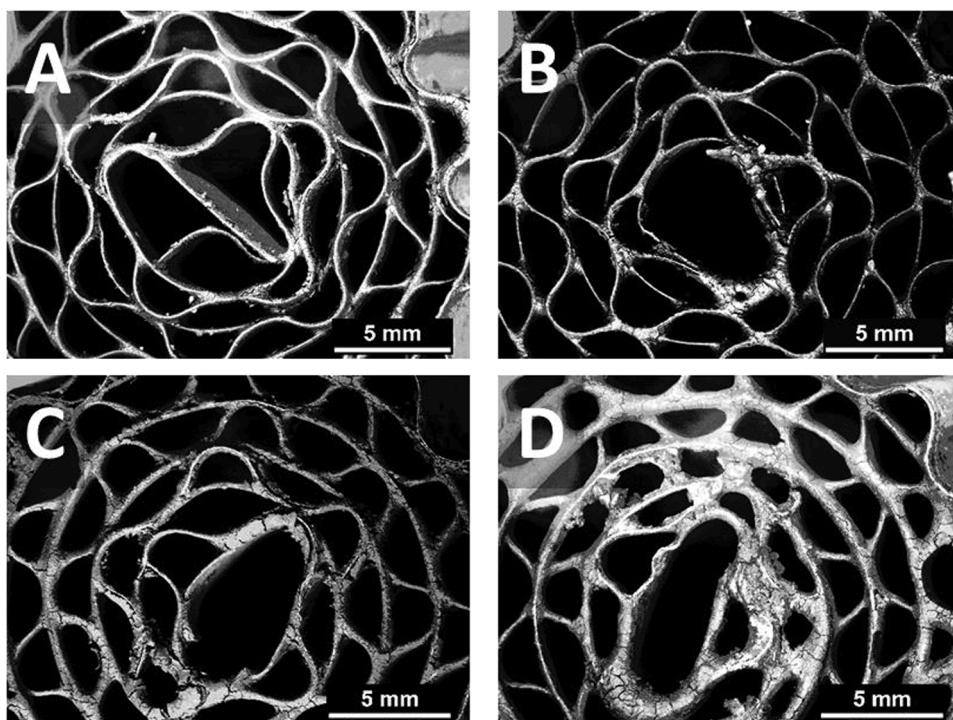
Fig. 2. Images of coated monoliths with a) CZA_10%Al$_2$O$_3$ b) CZA_33.3%Al$_2$O$_3$ c) CZA_33.3%ZnO and D) 33.3% SiO$_2$.
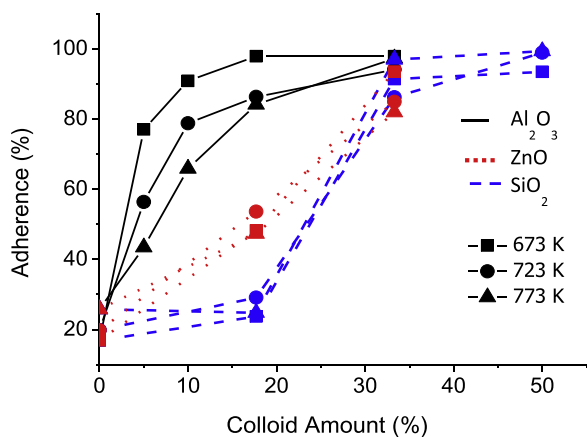

Fig. 3. Coating adherence varying colloids content and calcination temperature.

Fig. 4. XRD of colloidal alumina at different calcination temperatures

and the alumina whisker of Fecralloy® obtained after pre-treatment. Intermediate behaviour was observed using colloidal ZnO (compatible only with catalyst), and the less relevant results were obtained with slurries prepared with SiO$_2$ that do not present special compatibility, neither with the substrate nor with the catalyst. Therefore, chemical compatibility between the catalyst and the monolith surface is crucial increasing adherence with low binder content.

On the other hand, the calcination temperature (673-773 K) effect in adherence was studied (Fig. 3). A decrease in adherence was observed when the colloidal Al$_2$O$_3$ was used. By XRD analysis of the colloidal Al$_2$O$_3$ at different calcination temperatures (Fig. 4), it was found that the dried colloidal alumina presented a pseudo-boehmite phase (AlO(OH) or Al$_2$O$_3$·H$_2$O) that changed to γ-alumina at 773 K approximately. Calcination at 673 K resulted in an intermediate state between these two phases. Sánchez et al. [37] suggested that the Al(H$_2$O)$_4$OH]$_2^{4+}$ ions, which are present in boehmite, could react and form chemical bonds that improve the catalyst's adherence. Therefore, adherence decreases

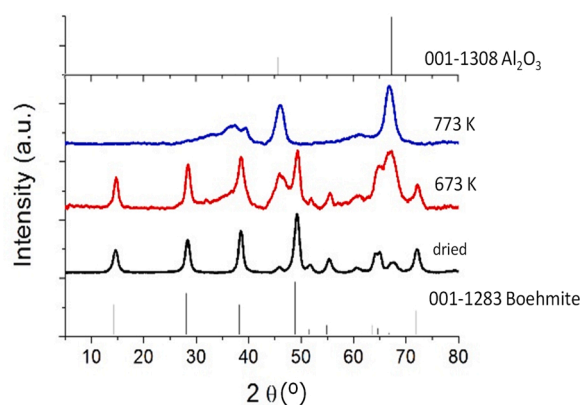when the OH groups are eliminated by increasing calcination temperatures (Fig. 3).

3.3. Effect of inorganic oxide colloids on the slurried catalyst

The effect of the inorganic colloids on the physicochemical properties of the CZA catalyst was analysed by obtaining the slurried catalyst samples by drying (373 K) and calcinating (673 K) the catalyst slurries (Table 1).

On the one hand, it can be seen in Table 3 that the textural properties of the slurried catalysts depend on the type and the amount of colloid added. Nevertheless, it seems that the colloids do not alter the textural properties of the parent catalyst because the texture of the slurried catalysts agrees with the weighted average of those of the individual components (catalyst and binder). As a result, the addition of the colloidal ZnO decreases the surface area of the slurried catalysts due to the low surface area that this colloid presents (19 m^2/g). However, adding colloidal Al$_2$O$_3$ increases the BET surface area, which could be attributed to the additional surface area provided by the colloidal

Table 3
Properties of different slurried catalysts.

Characterization technique	N$_2$-Adsorption			N$_2$O-RFC	H$_2$-TPR	XRD	
Sample Name	S$_{BET}$ (m^2/g)	V$_{PORE}$ (cm^3/g)	D$_{PORE}$ (nm)	Cu surface area (m^2/g $_{CZA}$)	Reducibility* (%)	CuO crystal size** (nm)	Cu° crystal size* (nm)
Parent catalyst	100	0.62	24	35.9	100	3.8	-
CZA_0%colloid	80.1	0.52	26	30.7	101	4.0	6.9
CZA_10%Al$_2$O$_3$	86.3	0.50	23	27.5	104	4.3	7.8
CZA_17.7%Al$_2$O$_3$	101	0.54	21	26.5	90	4.6	-
CZA_33.3%Al$_2$O$_3$	127	0.51	16	23.0	88	4.4	8.7
CZA_17.7%ZnO	55.2	0.38	27	21.3	85	4.6	-
CZA_33.3%ZnO	46.3	0.29	25	17.4	76	4.2	12.0
CZA_17.7%SiO$_2$	75.1	0.48	25	27.4	92	3.9	-
CZA_33.3%SiO$_2$	80.2	0.44	22	25.6	85	4.4	7.3
Colloidal Al$_2$O$_3$	204	0.31	6.2	-	-	-	-
Colloidal ZnO	19.1	0.11	24	-	-	-	-
Colloidal SiO$_2$	114	0.22	7.6	-	-	-	-

* The reducibility was measured by means of the H$_2$ consumption during TPR. In the case of our experimental conditions and the equipment adapted to measure integral monolith samples (high dead volume and therefore important widening of peaks), it allows us to obtain an accuracy in the measurement of hydrogen consumption no better than 10%.

** Estimated by Scherrer equation

alumina that doubles that of CZA.

On the other hand, the Cu metal surface area, the Cu° crystal size, and the catalyst reducibility were modified by incorporating the different colloids (Table 3). Both properties decrease with the addition of colloids. Such trends are more accentuated when colloidal ZnO is used (Table 3). However, even though significant modifications are not observed in the CuO crystal size by XRD, an increase in the Cu crystal size after reduction was observed by in-situ XRD analysis, in agreement with the decrease in the Cu surface area (Table 2) measured by N$_2$O-RFC.

Our results show that during the reduction process, the colloids seem to promote the sintering of the active phase. As can be seen below (Section 3.4.1), the decrease in the Cu surface area would lead to a decrease in activity. Some authors have observed that these additives can reduce the catalytic activity of the parent catalyst [17,19,38]. However, they suggest that this phenomenon is only due to a relative blocking of the active surface of the Cu, so it would be advisable to use the least necessary amount of colloids to promote adherence minimizing the alteration of catalytic properties [19].

The sample's acidity was also modified by adding the different inorganic oxide colloids (Fig. 5). Analysing the NH$_3$-TPD patterns, it can be seen that the parent catalyst and the slurried catalyst without colloids (CZA_0%colloid) presented similar acidity. However, when the colloids are added to the slurry formulation, the acidity changes depending on the colloid's nature and amount (Fig. 5). The colloidal alumina, which is well-known as an acid solid [39,40], presented higher acidity than the CZA catalyst (Fig. 5-B). Therefore, the addition of colloidal Al$_2$O$_3$ to the CZA catalyst increased the peak signal and, consequently, in the acidity of the final slurried catalyst (Fig. 5-B). A similar effect but less intense is

observed with colloidal SiO$_2$ (Fig. S3-A). When colloidal SiO$_2$ was added to the CZA catalysts, it slightly increased overall acidity (Fig. 5). In contrast, the colloidal ZnO presented negligible acidity (Fig. S3-B). Hence, using ZnO produced a sharp decrease in the overall acidity of the slurried catalyst (Fig. 5).

3.4. Methanol synthesis

First, methanol synthesis was studied with slurried samples to analyse the effect of binders on catalyst activity. The slurried catalysts were obtained by drying at 373 K and calcinating at 673 K catalyst slurries (Table 1). Later, the catalytic behaviour of structured catalysts coated with the selected slurry formulations was analysed.

3.4.1. Slurried catalyst activity

Samples with colloidal zinc oxide. Fig. 6A and Table 4 show the activity and selectivity of the powdered samples of the parent catalyst and the slurried catalysts without ZnO (0%) and with two different ZnO contents (17.7 and 33.3%).

The parent and the slurried catalysts activity without colloid is kind of low in comparison to other published studies. For example, García-Trenco et al. [41] at similar reaction conditions (pressure, temperature, and Lsyn/gCZA·h) obtained a CO conversion of around 20 %. However, the syngas composition of the cited research was 66% H$_2$/30% CO/4% CO$_2$; in our research, there is an absence of CO$_2$. It seems that the presence of CO$_2$ in the syngas composition improves the activity of Cu-based catalysts [42,43]. Moreover, hydrogenation of CO at equilibrium was shown to have a positive dependence on pressure, 50–100 bar
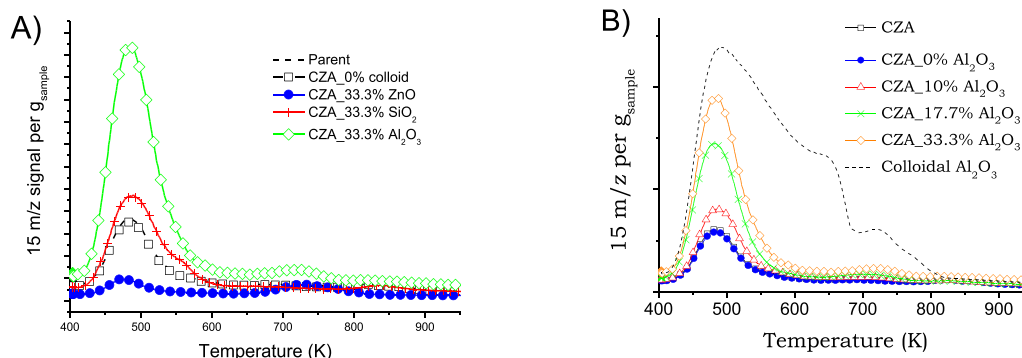

Fig. 5. NH$_3$-TPD curves monitored with m/z=15 by MS: (A) the effect of colloid type and (B) the effect of colloidal alumina amount.
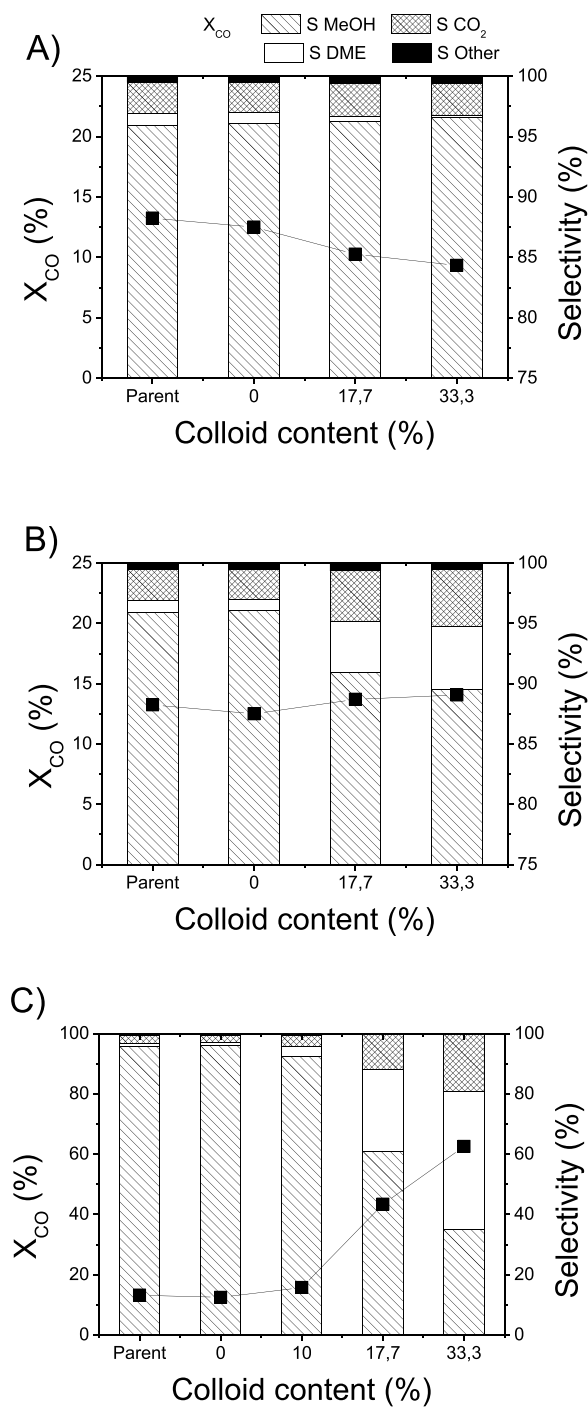
Fig. 6. Activity and selectivity in the methanol synthesis of samples with different colloid content: (A) ZnO, (B) SiO$_2$ and (C) Al$_2$O$_3$. Reaction conditions: 533 K, 4 MPa and 2.55 L$_{syngas}$/(g$_{CZA}$·h).

Table 4

CO conversion and selectivity value for the catalyst with different colloidal content at different space velocities. Reaction conditions: 533 K and 4 MPa.

Sample	SV (L$_{syn}$/ g$_{CZA}$·h)	X$_{CO}$ (%)	Selectivity (%)			
			MeOH	DME	CO$_2$	Other
CZA	2.55	13.2	95.9	0.98	2.63	0.49
CZA_0%	2.55	12.5	96.1	0.87	2.54	0.50
CZA_10%_Al$_2$O$_3$	2.55	15.8	92.5	3.29	3.68	0.52
CZA_17.7% _Al$_2$O$_3$	2.55	43.4	61.1	27.2	11.6	0.10
CZA_33.3% _Al$_2$O$_3$	2.55	62.6	34.9	45.8	19.1	0.10
CZA_17.7%_ZnO	1.2	17.6	96.0	0.53	2.7	0.73
	2.55	10.3	96.2	0.40	2.8	0.58
	5	5.2	96.2	0.31	3.0	0.57
CZA_33.3%_ZnO	1.2	15.6	96.3	0.17	2.8	0.74
	2.55	9.3	96.6	0.14	2.7	0.57
	5	4.9	96.4	0.15	2.9	0.51
CZA_17.7%_SiO$_2$	2.55	13.7	90.9	4.19	4.2	0.63
CZA_33.3%_SiO$_2$	2.55	14.1	89.5	5.27	4.7	0.52

reaction [26]. On the other hand, the colloidal ZnO also generated a slight decrease in the CO conversion, from 12 to 9%. A tendency was also observed at different space velocities (Table 4).

As seen before, adding the colloidal ZnO decreases the Cu surface area (Table 3), which could explain the decrease in the CO conversion. Nijhuis et al. [19] suggested that this could be due to the colloids' coverage of the metallic phase reducing the catalyst's activity. As said before, *in-situ* XRD analyses showed that the copper surface area decreased due to an increase in the Cu crystal size (Table 3). However, the decrease in CO conversion is significantly higher than that of the Cu surface area (Fig. 6-A and Table 4).

There is a great controversy concerning the mechanism of the methanol synthesis reaction and the role of zinc in this reaction [45]. Zn is widely thought to act as a promoter that improves Cu dispersion and reduces Cu sintering [45]. However, the reaction yield improves when ZnO is added to Cu-based catalysts [45–47]. Burch et al. [46] attributed this improvement to the role of ZnO as an H$_2$ reservoir. Hence, it would favour the hydrogenation of the reaction intermediates. On the contrary, Kanai *et al.* [47] propose that the activity improvement is due to the migration of ZnO$_x$ to the cooper surface that could generate CuZn alloys or Cu-O-Zn sites stabilising the Cu$^+$ ions.

Additional mixtures were studied to deepen the effect of colloidal ZnO on the CZA_33.3%ZnO catalyst's properties. First, a physical-mixture of powders of both compounds were separately pressed, grounded, and sieved (300-500 μm) and then mixed. Next, in the mechanical-mixture, powders of both compounds were initially mixed together and then pressed, grounded, and sieved to 300-500 μm. Finally, the slurried mixture was prepared in a water dispersion of both compounds, and then dried at 373 K and calcined at 673 K, pressed and sieved to 300-500 μm.

Fig. 7 and Table S1 show the prepared samples' catalytic and Cu surface area results with the different mixing methods. The results showed that the selectivity to DME is only altered by mixing both compounds with high interaction (slurried mixture), decreasing sharply (from 1.1 to 0.2 %). Despite reducing the Cu metal surface area due to increased contact between phases, CO conversion rose slightly in the mechanical mixture (Fig. 7, Table S1). The contact between phases in the physical mixture is insufficient to produce noticeable changes in the activity.

In contrast, intimate contact negatively affects the properties in the slurried mixtures. In the latter, the positive impact of ZnO is mitigated by the sharp decrease of the Cu metal surface area (Fig. 7, Table S1). However, the mechanical mixture allows for an intermediate contact while not causing a dramatic diminution of Cu surface area, which results in an improvement in CO conversion when the ZnO is added (Fig. 7, Table S1). Pori et al. [48] proposed that the increase in the methanol
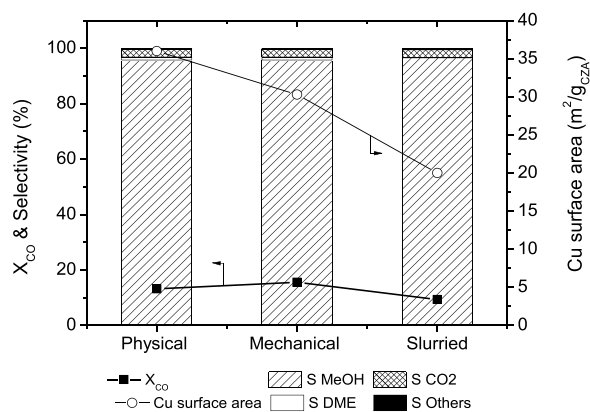
of pressure has to be used to obtain high conversions syngas to methanol [44]. Unfortunately, our experimental system did not allow experiments to be carried out with a pressure higher than 40 bar that would improve the activity of the catalyst.

The addition of colloidal zinc oxide produced slight changes in methanol synthesis. On the one hand, the use of ZnO resulted in a decrease in the selectivity to DME comparing with CZA_0% (Table 4). At the same reaction conditions, the DME selectivity decreases in this order: CZA_0%> CZA_17.7% > CZA_33.3%. This change in DME selectivity could be due to the basic character of the ZnO that neutralize the acid sites (Fig. 5) that are active in the methanol dehydration to DME

Fig. 7. Cu metal surface area and activity test of CZA_33.3%ZnO prepared with different mixing method. Reaction conditions: 533 K, 4 MPa and 2.55 $L_{syngas}/(g_{CZA}·h)$.

formation is due to a larger interface contact between Cu and ZnO. In the case of mechanical mixing, higher Cu-ZnO contact is possible than physical mixing. This contact is not as high as in the slurried system, where nanometric particles of the colloid can surround the Cu particles. However, the interaction in the case of the mechanical mixture can be high enough for the ZnO to partially block the surface of the Cu. Therefore, it seems that the type of contact between phases and consequently the interaction between them plays an important role.

The results show the demanding character of this reaction again, since the conversion of CO, i.e., the activity, is not directly proportional to the active surface area, the Cu surface area. As previously mentioned, different authors have indicated the positive role that Zn can play on the Cu in this reaction, increasing its specific activity (turnover number). Nevertheless, we have also seen that adding Zn in the form of colloid or physical mixtures can produce a partial coating of Cu that manifests itself on a lower active surface measured by N_2O-RFC (Table 1). Both effects are opposite as one increases the specific activity of Cu centres, but the other decreases the number of accessible surface centres. The activity, and, therefore, the CO conversion, will be proportional to the product of both turnover and number of active centres.

Samples with colloidal silica. The effect of adding colloidal silica to the slurried catalyst activity is shown in Fig. 6-B and Table 4. These results showed a slight increase in CO conversion (from 12 to 14%) with the silica content was observed. Meanwhile, the methanol selectivity decreased (from 96 to 89%), and the selectivity to dimethyl ether (DME) and CO_2 increased from 0.9 to 5.3% and 2.5 to 4.7%, respectively. The addition of colloidal silica produced a slight increase in the overall acidity of the sample (Fig. 1). Acid sites are active in the methanol dehydration reaction to DME, also producing water (Eq. (3)) [26]. Hence, the selectivity to methanol decreased, and the selectivity to DME increased. Simultaneously, the water production favours the water-gas shift (WGS) reaction, which increases CO_2 production.

$$2·CH_3OH \leftrightarrow CH_3OCH_3 + H_2O \qquad (3)$$

Samples with colloidal alumina. Fig. 6-C and Table 4 show the slurried catalyst's catalytic activity prepared with colloidal alumina. The higher the Al_2O_3 content is, the lower the methanol selectivity is and the higher the DME selectivity is. It is widely known the ability of alumina to dehydrate methanol to DME [40,49]. Alumina presents acid sites detected by the NH_3-TPD analysis (Figs. S2 and 5) that can produce methanol dehydration.

Apart from these changes in selectivity, the increase in colloidal Al_2O_3 content leads to increased CO conversion (Fig. 6-C). Furthermore,

methanol dehydration generates a consumption of methanol while it is formed; therefore, the methanol synthesis reaction is shifted, and the thermodynamic equilibrium limitation of this reaction is reduced [50, 51]. On the other hand, the dehydration of methanol to DME also generates water. Hence, the presence of this compound in the reactor favours the WGS reaction, and CO_2 is produced (Fig. 6-C) [50,51]. In conclusion, this "extra" acidity of the alumina leads to a decrease in the methanol yield.

The overall effect of alumina addition can be explained as the sum of opposed effects on activity and selectivity. On the one hand alumina produces a partial blockage of the Cu active surface that should produce a decrease in CO conversion. However, alumina provides also acid centres that dehydrate methanol as it is producing, which reduces the limitation of the thermodynamic equilibrium of methanol synthesis favouring greater conversion of CO. Our experimental results confirm that globally, the positive effect due to the transformation of methanol into DME is superior to the negative effect of a lower active surface of Cu to convert CO into methanol

The neutralization employing boric acid addition to the slurry formulation was studied to avoid the alumina's dehydration capacity. Mineral acids such as H_3BO_3 or H_3PO_4 are often used to modify alumina and to reduce the strength of the Lewis acid sites that this compound presents [27,52,53]. These mineral acids can avoid forming strong Lewis acid sites or reducing the adsorbate molecules' accessibility [27].

Fig. 8 shows the methanol synthesis activity and Cu surface area of the CZA_17.7%Al_2O_3 prepared with different H_3BO_3 amounts. The increase of boric acid content in the formulation produced a decrease in DME selectivity. However, even with the highest content studied (17.4 mmol of H_3BO_3/g Al_2O_3), DME selectivity ($\approx3\%$) did not reach the values of the parent catalyst ($\approx1\%$). Unfortunately, the CO conversion decreased as the H_3BO_3 content increased (Fig. 8-A) as expected due to the decrease of methanol dehydration, and consequently, acting against the displacement of the equilibrium. Nevertheless, the Cu surface area of the catalysts also decreased when the H_3BO_3 was added to the slurry (Fig. 8-B). Therefore, the addition of boric acid produces effects not only in selectivity but also on the active surface area and, therefore, in the activity. Consequently, this strategy did not help us to separate both effects and was abandoned.

3.4.2. Structured catalyst activity

The structured catalytic substrates were washcoated with the slurry formulations that presented the best correlation between good adherences with minor changes in catalytic properties, the CZA_10% Al_2O_3. Therefore, 1 g of this catalyst was deposited on Fecralloy® monolith of 289 cpsi (R4) and 2360 cpsi (R1). Structured samples were characterised (Table 5), and the catalytic activity was measured (Fig. 9).

In Table 5, it can be seen that the CZA_10%Al_2O_3 catalyst was successfully structured with similar physicochemical properties to that of the slurried catalyst. On the other hand, the structured catalysts also presented similar selectivities to the slurried catalyst, independent of the void fraction of the metallic monolith used (R4 or R1) (Fig. 9-A). However, the CO conversion values of the structured catalysts (R4 and R1) are slightly higher than that of the slurried catalyst (Fig. 9-A). The thickness of the layer is an essential factor in reactions with strong diffusion limitations, such as the Fischer-Tropsch reaction [15]. The average layer thickness was obtained by the coating density determination by Hg porosimetry and estimating the geometric surface area of the structured substrate. In this work, we have used two substrates with a geometric surface area twice the other (R1=521 cm^2 and R4= 207 cm^2) and, therefore, the catalytic layer thickness would be half from one to the other. As no differences in activity have been observed between the monoliths, it seems that there should be no diffusional problems in the case of the slurried catalyst that could explain the differences in activity.

The stability tests for up to 60 h of the monoliths were performed, presenting similar catalytic behavior (Fig. 10). However, we have tried
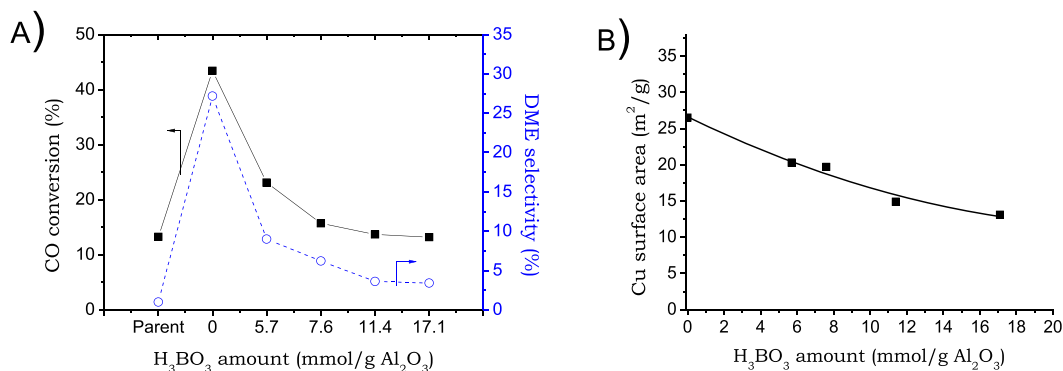
Fig. 8. Results of CZA_17.7%Al$_2$O$_3$: A) CO conversion and DME selectivity and B) Cu metal surface area with different H$_3$BO$_3$ contents.

Table 5
Textural properties and reducibility of the structured catalysts prepared with CZA_10%Al$_2$O$_3$.

Sample	Form	N$_2$-Adsorption			N$_2$O-RFC	H$_2$-TPR
		S$_{BET}$ (m^2/g)	V$_{Pore}$ (cm^3/g)	D$_{Pore}$ (nm)	Cu surface area (m^2/g$_{CZA}$)	Reducibility (%)
	Slurried	86	0.50	23	30.7	104
CZA_10% Al$_2$O$_3$	R4	87	0.45	21	31.1	103
	R1	92	0.44	19	32.1	105

to do these tests with the slurried catalyst without SiC (no isothermal bed), and the system is impossible to control thermally. Therefore, a correct comparison has not been possible.

Minimal temperature gradients (axial and radial) lower than ΔT=-3 °C inside monoliths are measured at 533 K (Fig. 9-B). The volumetric heat duty ($Q = \frac{-\Delta H_R^0 \cdot F_{CO}^{in} \cdot X_{CO}}{V_{reactor}}$, where ΔH_R^0 is the standard reaction enthalpy set to -90.6 kJ/mol$_{CO}$ and $V_{reactor}$ is the volume occupied by the structured catalyst) calculated in the experiments with the monolithic reactors was lower than 30 kW/m^3, being a moderate value. In our previous works using similarly structured reactors for highly exothermic reactions (DME synthesis [54] and FTS [15,55]), the temperature differences were significant when using FeCrAl monoliths when Q is higher than 160 kW/m^3.

To the best of our knowledge, there is little bibliography about structuring Cu/ZnO/Al$_2$O$_3$ catalyst for methanol synthesis. For example, Montebelli et al. [3] tried to coat Cu/ZnO/Al$_2$O$_3$ catalyst in metallic

open-cell foams, but a decrease in activity was observed, which was attributed to the slurry preparation, calcination, or both treatments. In contrast, Phan et al. [4] achieved the preparation of a Cu-based catalyst on Fecralloy® monoliths with good activity performances. What is more important, these structured catalysts presented better activity than the corresponding powder catalyst. The authors suggested that the superior performance of the structured catalyst could be related to the better thermal properties of the metallic substrates: the axial temperature gradient in a fixed bed reactor configuration reached up to 10°C, being less than 1°C in the case of the structured catalyst [4].

4. Conclusion

The structuration of the CZA catalyst was successfully obtained by the washcoating method. When preparing a suitable formulation of this catalyst in aqueous media, the suspension's pH must be considered to produce high repulsion between particles while preserving their structure.

The use of inorganic colloids (ZnO, SiO$_2$, and Al$_2$O$_3$) is crucial for obtaining good adherence between the catalyst layer and the monolith. The small size of the colloidal particles improves adherence by increasing the adhesive and cohesive properties of the catalyst layer and substrate. Moreover, the chemical compatibility of the colloid with the catalyst and the monolith scale controls the amount of colloid required for good adherence. However, colloids also produce a negative effect on the activity since they partially cover the copper surface and decrease its reducibility, reducing thus their ability to convert CO into methanol. Therefore, both effects, positive and negative must be balanced, using the least amount of colloid necessary to enhance the adhesion of the catalytic layer to the substrate, thus minimizing the loss of activity due
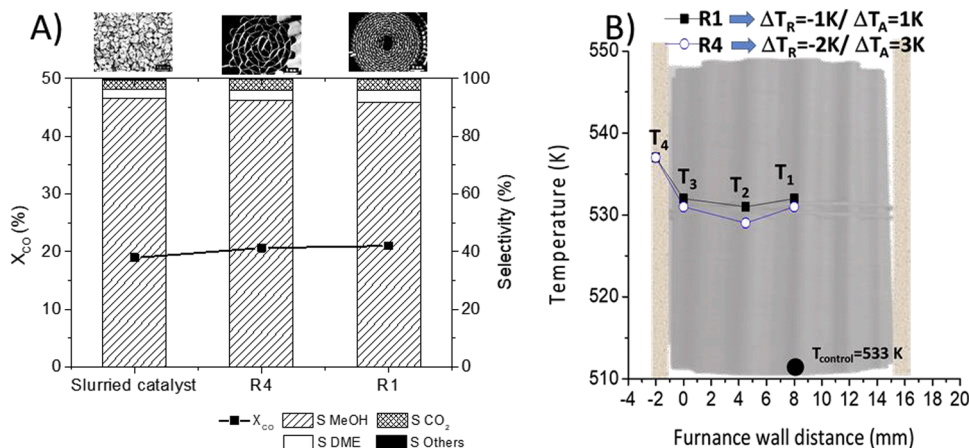

Fig. 9. Activity test (A) and temperature gradients (B) of structured catalyst coated with 1 g of CZA_10%Al$_2$O$_3$ at 533 K and 4 MPa at space velocity of 2.55 L$_{syn}$/(g$_{CZA}$·h). ΔT$_R$= T$_{control}$ −T$_3$ and ΔT$_A$= T$_{control}$ −T$_1$.
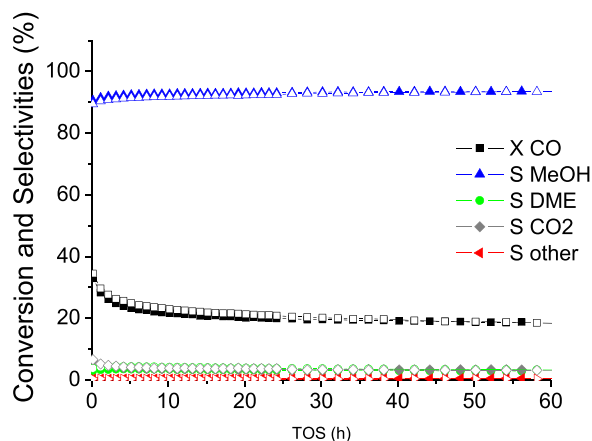
Fig. 10. Activity test of structured catalyst of CZA_10%Al2O3 sample in Fecralloy® monoliths of R1_18. (Filled symbols) and R4_46.5μm (empty symbols). Reaction conditions: 260 °C, 40 bar and 2.55 Lsyn/gCZA·h. Coated catalyst 1 g.

to the loss of copper surface.

Significant colloid content (>33.3%) dramatically decreases the Cu metallic surface area and reducibility. Moreover, the acidity of colloids like Al_2O_3 and SiO_2 is able modify the selectivity because it is able to dehydrate the methanol produced to DME (not desired product), and this effect is proportional to the colloid content. On the other hand, changes in selectivity can also modify the global conversion of CO. Methanol synthesis is a thermodynamically balanced reaction, so the disappearance of methanol produced favours the displacement of the equilibrium to the right and therefore increases the conversion of CO.

When alumina is used as a colloid, the positive effect in the conversion of CO due the displacement of the equilibrium by methanol consumption prevails on the negative effect produced by the partial blockage of the copper surface. In addition, the positive effect on adhesion is obtained with lower alumina content (10%) than in the case of silica or zinc oxide. CZA_10%Al$_2$O$_3$ formulation showed excellent activity when used to coat Fecralloy® monoliths with different cell densities.

CRediT authorship contribution statement

Iñigo Pérez-Miqueo: Conceptualization, Methodology, Validation, Investigation, Writing – original draft. **Oihane Sanz:** Conceptualization, Methodology, Validation, Investigation, Writing – original draft, Writing – review & editing, Visualization, Supervision, Project administration, Funding acquisition. **Mario Montes:** Conceptualization, Methodology, Validation, Investigation, Supervision, Project administration, Funding acquisition.

Declaration of Competing Interest

None.

Data availability

No data was used for the research described in the article.

Acknowledgements

Supplementary materials

Supplementary material associated with this article can be found, in the online version, at doi:10.1016/j.cep.2022.109210.

References

[1] R. Fan, M. Kyodo, L. Tan, X. Peng, G. Yang, Y. Yoneyama, R. Yang, Q. Zhang, N. Tsubaki, Preparation and application of Cu/ZnO catalyst by urea hydrolysis method for low-temperature methanol synthesis from syngas, Fuel Process. Technol. 167 (2017) 69, https://doi.org/10.1016/j.fuproc.2017.06.026.

[2] Visconti, C.G.; Montebelli, A.; Groppi, G.; Tronconi, E.; Kohle, S. in A. Basile, F. Dalena (Eds.). *Methanol: Science and Engineering*. Elsevier, the Netherlands, 2018, pp. 519-538. 10.1016/B978-0-444-63903-5.00019-4.

[3] A. Montebelli, C.G. Visconti, G. Groppi, E. Tronconi, S. Kohler, H.J. Venvik, R. Myrstad, Washcoating and chemical testing of a commercial Cu/ZnO/Al2O3 catalyst for the methanol synthesis over copper open-cell foams, Appl. Catal. A Gen. 481 (2014) 96, https://doi.org/10.1016/j.apcata.2014.05.005.

[4] X.K. Phan, H. Bakhtiary-Davijany, R. Myrstad, P. Pfeifer, H.J. Venvik, A. Holmen, Preparation and performance of Cu-based monoliths for methanol synthesis, Appl. Catal. A: Gen. 405 (2011) 1, https://doi.org/10.1016/j.apcata.2011.07.005.

[5] K.A. Ali, A.Z. Abdullah, A.R. Mohamed, Recent development in catalytic technologies for methanol synthesis from renewable sources: a critical review, Renew. Sust. Energy Rev. 44 (2015) 508, https://doi.org/10.1016/j.rser.2015.01.010.

[6] S.G. Jadhav, P.D. Vaidya, B.M. Bhanage, J.B. Joshi, Catalytic carbon dioxide hydrogenation to methanol: a review of recent studies, Chem. Eng. Res. Des. 92 (2014) 2557, https://doi.org/10.1016/j.cherd.2014.03.005.

[7] D. Sheldon, Industry and sustainability, Johnson Matthey Technol. Rev. 61 (2017) 172, https://doi.org/10.1595/205651317X695857.

[8] C. Ahoba-Sam, U. Olsbye, K.J. Jens, Low temperature methanol synthesis catalyzed by copper nanoparticles, Catal. Today 299 (2018) 112, https://doi.org/10.1016/j.cattod.2017.06.038.

[9] A. Prašnikar, D.L. Jurković, B. Likozar, Reaction Path Analysis of CO2 Reduction to Methanol through Multisite Microkinetic Modelling over Cu/ZnO/Al2O3 Catalysts, Appl. Catal. B 292 (2021), 120190, https://doi.org/10.1016/j.apcatb.2021.12019.

[10] J. Ott, V. Gronemann, F. Pontzen, R.E. Fiedle, G. Grossmann, DB. Kersebohm, G. Weiss, C. Witte, Methanol, in: Ullmann's Encycl. Ind. Chem., 4, Wiley-VCH Verlag GmbH & Co. KGaA, Germany, 2012, pp. 25–48, https://doi.org/10.1002/14356007.a16_465.pub3.

[11] J-P. Lange, Methanol synthesis: a short review of technology improvements, Catal. Today 64 (2001) 3, https://doi.org/10.1016/S0920-5861(00)00503-4.

[12] Sanz, O.; Echave, F.J.; Romero-Sarria, F.; Odriozola, J.A.; Montes, M. in Gandía, L. M.; Arzamendi, G.; Diéguez P.M. (Eds.). *Renewable Hydrogen Technologies*. Elsevier. The Netherlands, 2013, pp. 201-224. http://dx.doi.or/10.1016/B978-0-444-56352-1.00009-X.

[13] A. Montebelli, C.G. Visconti, G. Groppi, E. Tronconi, S. Kohler, Optimization of compact multitubular fixed-bed reactors for the methanol synthesis loaded with highly conductive structured catalysts, Chem. Eng. J. 255 (2014) 257, https://doi.org/10.1016/j.cej.2014.06.050.

[14] O. Sanz, I. Velasco, I. Pérez-Miqueo, R. Poyato, J.A. Odriozola, M. Montes, Intensification of hydrogen production by methanol steam reforming, Int. J. Hydrog. Enerergy 41 (2016) 5250, https://doi.org/10.1016/j.ijhydene.2016.01.084.

[15] A. Egaña, O. Sanz, D. Merino, X. Moriones, M. Montes, Fischer–tropsch synthesis intensification in foam structures, Ind. Eng. Chem. Res. 57 (2018) 10187, https://doi.org/10.1021/acs.iecr.8b01492.

[16] A. Montebelli, C.G. Visconti, G. Croppi, E. Tronconi, C. Cristiana, C. Ferreira, S. Kohler, Methods for the catalytic activation of metallic structured substrates, Catal. Sci. Technol. 4 (2014) 2846, https://doi.org/10.1039/C4CY00179F.

[17] F.J. Echave, O. Sanz, M. Montes, Washcoating of microchannel reactors with PdZnO catalyst for methanol steam reforming, Appl. Catal. A Gen. 474 (2014) 159, https://doi.org/10.1016/j.apcata.2013.07.058.

[18] P. Ávila, M. Montes, E.E. Miró, Monolithic reactors for environmental applications: a review on preparation technologies, Chem Eng. J. 109 (2005) 11, https://doi.org/10.1016/j.cej.2005.02.025.

[19] T.A. Nijhuis, A.E.W. Beers, T. Vergunst, I. Hoek, F. Kapteijn, J.A. Moulijn, Preparation of monolithic catalysts, Catal. Rev. 43 (2001) 345, https://doi.org/10.1081/CR-120001807.

[20] J.M. Zamaro, M.A. Ulla, E.E. Miró, Zeolite washcoating onto cordierite honeycomb reactors for environmental applications, Chem. Eng. J. 106 (2005) 25, https://doi.org/10.1016/j.cej.2004.11.003.

[21] H. Pérez, P. Navarro, M. Montes, Deposition of SBA-15 layers on Fecralloy monoliths by washcoating, Chem. Eng. J. 158 (2010) 325, https://doi.org/10.1016/j.cej.2010.01.032.

[22] N.R. Peela, A. Mubayi, D. Kunzru, Washcoating of γ-alumina on stainless steel microchannels, Catal. Today 147S (2009) S17, https://doi.org/10.1016/j.cattod.2009.07.026.

[23] V.G. Milt, S. Ivanova, O. Sanz, M.I. Dominguez, A. Corrales, J.A. Odriozola, M. A. Centeno, Au/TiO2 supported on ferritic stainless steel monoliths as CO oxidation

catalysts, Appl. Surf. Sci. 270 (2013) 169, https://doi.org/10.1016/j.apsusc.2012.12.159.

[24] C. Baltes, S. Vukojevi, F. Schüth, Correlations between synthesis, precursor, and catalyst structure and activity of a large set of CuO/ZnO/Al₂O₃ catalysts for methanol synthesis, J. Catal. 258 (2008) 334, https://doi.org/10.1016/j.jcat.2008.07.004.

[25] L.R. Chapman, Enhanced oxide whisker growth on cold-rolled aluminum-containing stainless steel foil. U.S. Patent 4,318,828, 1982.

[26] J.J. Spivey, Review: dehydration catalysts for the methanol/dimethyl ether reaction, Chem. Eng. Commun. 110 (1991) 123, https://doi.org/10.1080/00986449108939946.

[27] R.I. Samoilova, S.A. Dikanov, A.V. Fionov, A.M. Tyryshkin, E.V. Lunina, M.K. Bowman, Pulsed EPR study of orthophosphoric and boric acid modified γ-alumina, J. Phys. Chem. 100 (1996) 17621, https://doi.org/10.1021/jp961873b.

[28] G.C. Chinchen, C.M. Hay, H.D. Vandervell, K.C. Waugh, The measurement of copper surface areas by reactive frontal chromatography, J. Catal. 103 (1987) 79, https://doi.org/10.1016/0021-9517(87)90094-7.

[29] Yasaki, S.; Yoshino, Y.; Ihara, K.; Ohkubo, K. Method of manufacturing an exhaust gas purifying catalyst. U.S. Patent 5,208,206, 1993.

[30] J.M. Zamaro, M.A. Ulla, E.E. Miró, The effect of different slurry compositions and solvents upon the properties of ZSM5-washcoated cordierite honeycombs for the SCR of NOx with methane, Catal. Today 86 (2005) 107–108, https://doi.org/10.1016/j.cattod.2005.07.066.

[31] F.J. Echave Lozano, Reactores catalíticos de microcanales para el reformado de alcoholes, University of the Basque Country, San Sebastian, ES, 2011. Ph. D. Dissertation.

[32] B.J. Hathaway, A.A.G. Tomlinson, Copper (II) ammonia complexes, Coord. Chem. Rev. 5 (1) (1970), https://doi.org/10.1016/S0010-8545(00)80073-9.

[33] J.W. Bae, S.H. Kang, Y.J. Lee, K.W. Jun, Effect of precipitants during the preparation of Cu-ZnO-Al₂O₃/Zr-ferrierite catalyst on the DME synthesis from syngas, Ind. Eng. Chem. Res. 15 (2009) 566, https://doi.org/10.1016/j.jiec.2009.01.014.

[34] C. Agrafiotis, A. Tsetsekou, The effect of powder characteristics on washcoat quality. Part I: alumina washcoats, J. Eur. Ceram. Soc. 20 (2000) 815, https://doi.org/10.1016/S0955-2219(99)00218-6.

[35] R.M. Heck, R.J. Farrauto, Catalyst characterization. Catalytic Air Pollution Control – Commercial Technology 29–47, John Wiley& Sons, New York, 1995.

[36] S. Zhao, J. Zhang, D. Weng, X. Wu, A method to form well-adhered γ-Al₂O₃ layers on FeCrAl metallic supports, Surf. Coat. Technol. 167 (2003) 97, https://doi.org/10.1016/S0257-8972(02)00859-9.

[37] J.F. Sánchez, O.J. González Bello, M. Montes, G.M. Tonetto, D.E. Damiani, Pd/Al₂O₃-cordierite and Pd/Al₂O₃-Fecralloy monolithic catalysts for the hydrogenation of sunflower oil, Catal. Commun. 10 (2009) 1446, https://doi.org/10.1016/j.catcom.2009.03.016.

[38] A. Galarneau, A. Sachse, B. Said, C.-H. Pelisson, P. Boscaro, N. Brun, L. Courtheoux, N. Olivi-Tran, B. Coasne, F. Fajula, Hierarchical porous silica monoliths: A novel class of microreactors for process intensification in catalysis and adsorption, C. R. Chim. 19 (2016) 231, https://doi.org/10.1016/j.crci.2015.05.017.

[39] F.S. Ramos, A.M. Duarte de Farias, L.E.P. Borge, J.L. Monteiro, M.A. Fraga, E.F. Sousa-Aguiar, L.G. Appel, Role of dehydration catalyst acid properties on one-

step DME synthesis over physical mixtures, Catal. Today 101 (2005) 39, https://doi.org/10.1016/j.cattod.2004.12.007.

[40] F. Song, Y. Tan, H. Xie, Q. Zhang, Y. Han, Direct synthesis of dimethyl ether from biomass-derived syngas over Cu–ZnO–Al₂O₃–ZrO₂(x)/γ-Al₂O₃ bifunctional catalysts: effect of Zr-loading, Fuel Process. Technol. 126 (2014) 88, https://doi.org/10.1016/j.fuproc.2014.04.021.

[41] A. García-Trenco, A. Vidal-Moya, A. Martínez, Study of the interaction between components in hybrid CuZnAl/HZSM-5 catalysts and its impact in the syngas-to-DME reaction, Catal. Today 179 (2012) 43, https://doi.org/10.1016/j.cattod.2011.06.034.

[42] J.S. Lee, K.H. Lee, S.Y. Lee, Y.G. Kim, A comparative study of methanol synthesis from CO₂/H₂ and CO/H₂ over a Cu/ZnO/Al₂O₃ catalyst, J. Catal. 144 (1993) 414, https://doi.org/10.1006/jcat.1993.1342.

[43] R. Zao-Xin, J. Wang, J. Lin-Ying, L. Da-Shun, Effect of carbon dioxide on methanol synthesis over different catalysts, Appl. Catal. 49 (1989) 83, https://doi.org/10.1016/S0166-9834(00)81424-4.

[44] G. Leonzio, Methanol synthesis: optimal solution for a better efficiency of the process, Processes 6 (2018) 20, https://doi.org/10.3390/pr6030020.

[45] T. Matsuhisa, J.J. Spivey, Catalysis: Volume 12, The Royal Society of Chemistry, United Kingdom, 1996, pp. 1–20, https://doi.org/10.1039/9781847553249-00001.

[46] R. Burch, S.E. Golunski, M.S.J Spencer, The role of copper and zinc oxide in methanol synthesis catalysts, Chem. Soc. Faraday Trans. 86 (1990) 2683, https://doi.org/10.1039/FT9908602683.

[47] Y. Kanai, T. Watanabe, T. Fujitani, T. Uchijima, J. Nakamura, The synergy between Cu and ZnO in methanol synthesis catalysts, Catal. Lett. 38 (1996) 157–163, https://doi.org/10.1007/BF00806562.

[48] M. Poria, B. Likozara, M. Marinšekb, Z. Crnjak Orel, Fuel Process. Technol. 39 (2016) 146, https://doi.org/10.1016/j.fuproc.2016.02.021.

[49] S.S. Akarmazyan, P. Panagiotopoulou, A. Kambolis, C. Papadopoulou, D. Kondarides, Methanol dehydration to dimethylether over Al₂O₃ catalysts, Appl. Catal. B 136 (2014) 145, https://doi.org/10.1016/j.apcatb.2012.11.043.

[50] C. Arcoumanis, C. Bae, R. Crookes, E. Kinoshita, The potential of di-methyl ether (DME) as an alternative fuel for compression-ignition engines: a review, Fuel 87 (2008) 1014, https://doi.org/10.1016/j.fuel.2007.06.007.

[51] T.A. Semelsberger, R.L. Borup, H.L. Greene, Dimethyl ether (DME) as an alternative fuel, J. Power Sources 156 (2006) 497, https://doi.org/10.1016/j.jpowsour.2005.05.082.

[52] S. Sato, M. Kuroki, T. Sodesawa, F. Nozaki, G.E. Maciel, J. Mol. Catal. A Chem. 104 (1995) 171, https://doi.org/10.1016/1381-1169(95)00105-0.

[53] F.M. Bautista, J.M. Campelo, A. García, D. Luna, J.M. Marinas, M.C. Moreno, A.A. Romero, Acidity and catalytic activity of AlPO₄–B₂O₃ and Al₂O₃–B₂O₃ (5–30 wt % B₂O₃) systems prepared by impregnation, Appl. Catal. A Gen. 170 (1998) 159, https://doi.org/10.1016/S0926-860X(98)00046-5.

[54] I. Pérez-Miqueo, O. Sanz, M. Montes, Highly conductive structured catalytic reactors for one-step synthesis of dimethyl ether, Ind. Eng. Chem. Res. 60 (2021) 6676, https://doi.org/10.1021/acs.iecr.0c05821.

[55] D. Merino, O. Sanz, M. Montes, Effect of the thermal conductivity and catalyst layer thickness on the Fischer–Tropsch synthesis selectivity using structured catalysts, Chem. Eng. J. 327 (2017) 1033, https://doi.org/10.1016/j.cej.2017.07.003.